

# $^{31}\text{P}$ NMR Investigation of the Superconductor LiFeP ( $T_c = 5$ K)

HUIYUAN MAN, SHENGLI GUO, GUOXIANG ZHI, XIN GONG, QUAN WANG, CUI DING, YANKANG JIN AND FANLONG NING<sup>(a)</sup>

*Department of Physics, Zhejiang University - Hangzhou 310027, China*

PACS 74.70.-b – Superconducting materials

PACS 76.60.-k – Nuclear magnetic resonance and relaxation

**Abstract** – We investigate the static and dynamic spin susceptibility of the “111” type Fe-based superconductor LiFeP with  $T_c \sim 5$  K through the measurement of Knight shift  $^{31}\text{K}$  and the spin-lattice relaxation rate  $\frac{1}{T_1}$  at  $^{31}\text{P}$  site by nuclear magnetic resonance. The constant  $^{31}\text{K}$ , small magnitudes of  $\frac{1}{T_1 T}$ , along with the resistivity  $\rho \sim T^2$  all point to the weak spin correlations in LiFeP.  $\frac{1}{T_1 T}$  display small enhancement toward  $T_c$ , indicating that the superconductivity is intimately correlated with the antiferromagnetic spin fluctuations.

**Introduction.** – The discovery of superconductivity with  $T_c = 26$  K in the layered structure  $\text{La}(\text{O}_{1-x}\text{F}_x)\text{FeAs}$  ( $x = 0.05 \sim 0.12$ ) [1] has generated great interest into the research of Fe-based high temperature superconductors. Over the past six years, hundreds of Fe-based superconductors have been reported and the list has expanded rapidly from the original  $\text{LaFeAsO}$  “1111” structure [1, 2] to  $\text{MFe}_2\text{As}_2$  (M stands for alkali earth metal) “122” family [3],  $\text{MFeAs}$  (M stands for alkali metal) “111” family [4], the iron chalcogenide  $\text{FeSe}$  “11” family [5], the “42622” family [6] and the “32522” family [7] etc. Despite the different crystalline structures, accumulating experimental and theoretical results have pointed to the unconventional superconducting pair symmetry of these Fe-based superconductors, and the common physical properties they shared [8, 9].

LiFeP is one of the prototypical superconductor in the “111” family, which was found to become superconducting below  $T_c \sim 6$  K [10]. In addition to the much lower  $T_c$ , LiFeP has some properties different from other “111”-type superconductors LiFeAs [11] and NaFeAs [12]. For example, the measurements of magnetic penetration depth  $\lambda$  have indicated a nodal superconducting order parameter for LiFeP [13], different from the fully gapped state observed for LiFeAs [13]. Furthermore, no magnetic or structural transition has been observed in LiFeP and LiFeAs, but a structural transition at  $T_s = 57$  K [14] and a SDW magnetic transition at  $T_{SDW} = 45$  K [15] have been ob-

served in NaFeAs. On the other hand, it has been shown in LiFeAs by NMR (Nuclear Magnetic Resonance) that the antiferromagnetic spin fluctuations are strongly enhanced toward  $T_c$  [16]. The feature of antiferromagnetic spin fluctuations enhancement toward  $T_c$  has been observed in other Fe-based families [17–21], which provides convincing experimental evidences that the superconductivity is intimately correlated to the antiferromagnetic spin fluctuations. To the best of our knowledge, no NMR investigations of LiFeP have been reported. It will be interesting to investigate the spin dynamics and examine if such feature exists in the superconducting LiFeP.

In this paper, we conduct NMR measurement on a polycrystalline sample in the paramagnetic state. We measured the static susceptibility and the spin dynamics through the Knight shift and  $\frac{1}{T_1 T}$  measurements at  $^{31}\text{P}$  site, respectively. We found that the static susceptibility is temperature independent throughout the measured temperature range of 4.2 K and 280 K. While the magnitude of antiferromagnetic fluctuations is almost an order of magnitude smaller than those of LiFeAs [16], a weak enhancement toward  $T_c$  is observed. This indicates that the superconductivity is intimately correlated with the antiferromagnetic spin fluctuations despite the lower  $T_c$  of LiFeP.

**Experiments.** – The LiFeP polycrystalline specimens were synthesized by the solid state reaction method. The pallets of mixed high-purity Fe (99.9 %) and P (99 %) powders (Alfa Aesar) were sealed in an evacuated quartz

<sup>(a)</sup>E-mail: ningfl@zju.edu.cn

tube and heated to 800 °C for 10 hours to prepare the intermediate product FeP. FeP were then mixed with Li ingots (Alfa Aesar, 99.9%) with nominal concentration and heated to 800 °C for 30 h. The specimens were then cooled down to room temperature with the furnace shutting off. The handling of materials were performed in a high-purity argon filled glove box (the percentage of O<sub>2</sub> and H<sub>2</sub>O ≤ 0.1 ppm), to protect it from exposing to air. The color of the sample was shiny black, indicating the good crystallization.

The polycrystals were characterized by the X-ray powder diffraction and the dc magnetization with a Quantum Design superconducting quantum interference device (SQUID). The temperature dependence of electrical resistivity was measured on a thin bar-shaped sample (3.78 mm×1.02 mm ×1.08 mm) in a Cryogenic Mini-CFM system by a standard four-probe method. We conducted the <sup>31</sup>P NMR measurements by using the standard pulsed NMR techniques. We obtained the NMR spin echo signal by applying 90°-180° pulses in a fixed external field of  $B_{ext} = 4.65$  Tesla.

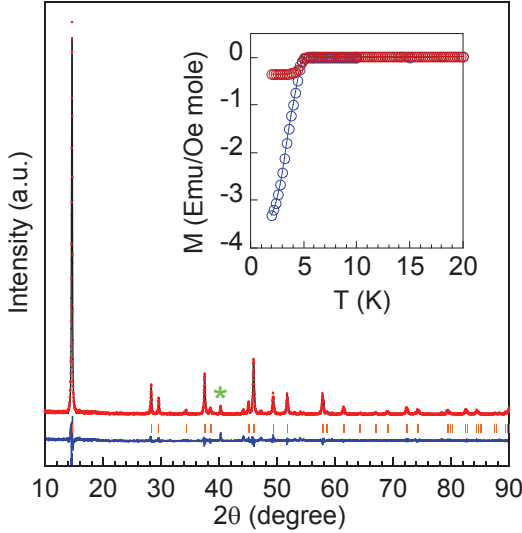


Fig. 1: (Color online) Powder X-ray diffraction pattern of LiFeP. Star marks the small amount of Fe<sub>2</sub>P impurity. The inset displays the dc susceptibility of LiFeP sample in both ZFC and FC mode, and the diamagnetic signals indicate that  $T_c \sim 5$  K.

**Results and discussion.** — In Fig. 1, we show the powder X-ray diffraction pattern of LiFeP polycrystal. The diffraction peaks can be well indexed into a Cu<sub>2</sub>Sb type tetragonal structure with  $P4/nmm$  symmetry [10], which is the same as the other two “111” type iron-based superconductor LiFeAs [11] and NaFeAs [12]. A careful inspection indicates that small amount of Fe<sub>2</sub>P exists at  $2\theta = 40.28^\circ$ . Fe<sub>2</sub>P is a ferromagnetic material with Curie temperature more than 200 K [22]. This small amount of impurity will not affect our NMR measurements of the intrinsic properties of LiFeP since NMR is a local and

site-selective microscopic probe and we conducted NMR measurements at <sup>31</sup>P site of LiFeP. The lattice constants are  $a = 3.6938\text{\AA}$  and  $c = 6.0446\text{\AA}$ , which are consistent with the previous reported values [10]. Compared to the values of  $a = 3.9494\text{\AA}$  and  $c = 7.0396\text{\AA}$  for NaFeAs [12], and  $a = 3.77\text{\AA}$  and  $c = 6.36\text{\AA}$  for LiFeAs [11], both the ab-plane and the c axis of LiFeP shrink to some extent. The smaller lattice constants of LiFeP have been attributed to much smaller atomic size of Li and P atoms than that of Na and As. In the inset of Fig. 1, we show the dc magnetic susceptibility of LiFeP sample measured in both ZFC and FC condition with an applied field of 20 Oe. The diamagnetic signals confirm the superconductivity takes place at  $\sim 5$  K. The superconducting volume fraction reaches 100% for ZFC mode at 2 K after the correction of the demagnetizing factors. The bulk superconductivity has also been confirmed through the observation of abrupt change of conduction frequency in a NMR coil.

In Fig. 2, we show the temperature dependence of electrical resistivity of LiFeP. The resistivity data indicates a sharp superconducting transition temperature at  $\sim 5$  K. The residual resistivity in our specimen is  $5.7 \mu\Omega\cdot\text{cm}$ , which is smaller than the value of previous reports [10, 23], indicating the good quality of our polycrystalline specimen. We plot the resistivity versus  $T^2$  in the temperature range of 5 K and 40 K, and a linear dependence has been observed. We do not observe anomalies corresponding to the SDW transition or structural transition that have been observed in the NaFeAs superconductor [12, 14, 15]. This situation is similar to the case of LiFeAs [11] where no anomalies have been observed in the curves of both electrical resistivity and magnetic susceptibility.

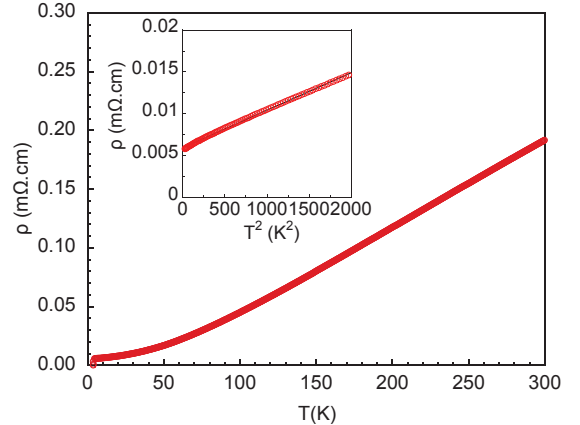


Fig. 2: (Color online) Temperature-dependent electrical resistivity for LiFeP polycrystalline sample, showing superconducting transition at  $\sim 5$  K. The inset shows the expanded  $\rho(T^2)$  data, suggesting a linear behavior at low temperature; The black solid line is a fitting line with the function  $\rho = \rho_0 + AT^2$  with  $\rho_0 = 0.0057 \text{ m}\Omega\cdot\text{cm}$  and  $A = 4.5 \times 10^{-6} \text{ m}\Omega\cdot\text{cm}/\text{K}^2$ .

We carried out the <sup>31</sup>P NMR lineshapes measurements under the field of  $B_{ext} = 4.65$  Tesla. This field is much higher than the second critical field  $\sim 2$  Tesla of LiFeP

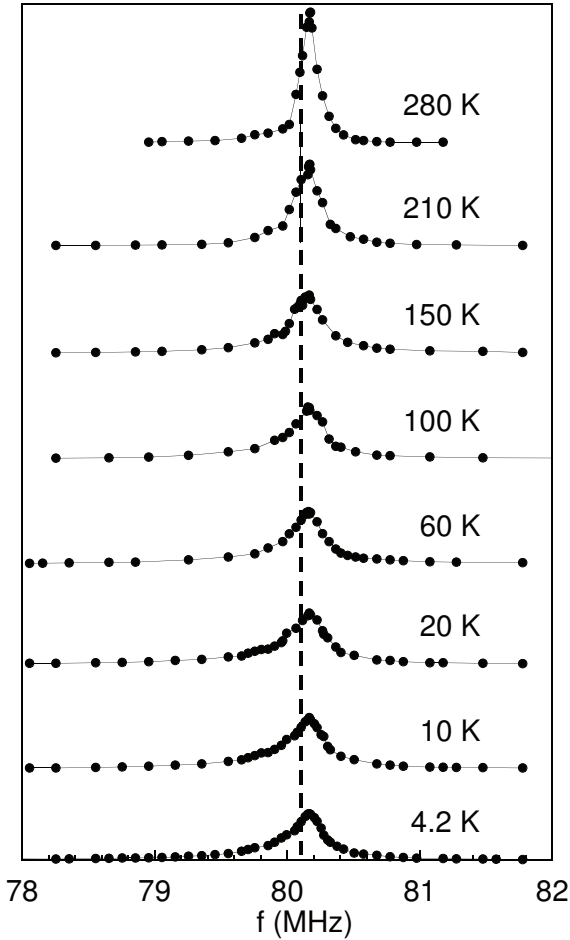


Fig. 3:  $^{31}\text{P}$  lineshapes of LiFeP measured over a wide temperature range from 4.2 K to 280 K under a field of 4.65 Tesla. The dashed line marks the position of  $^{31}\text{K} = 0$ .

[24, 25], and therefore it is in the paramagnetic state.  $^{31}\text{P}$  has a nuclear spin  $I = \frac{1}{2}$  with a gyromagnetic ratio of  $^{31}\gamma_n/2\pi = 17.235\text{ MHz/Tesla}$ . We would observe a single resonance frequency for each individual  $^{31}\text{P}$  site since there is no nuclear quadrupole interaction. In Fig. 3, we display the temperature dependence of  $^{31}\text{P}$  lineshapes for LiFeP from 280 K to the base temperature of 4.2 K. Only one resonance frequency is observed at  $f \sim 80.166\text{ MHz}$ , indicating that all  $^{31}\text{P}$  atoms are in the same magnetic and electrical environment. For a naked nuclei, the center of resonance frequency is  $f_0 = (^{31}\gamma_n/2\pi) \times B_{ext} = 80.143\text{ MHz}$ . It is the local field arising from the hyperfine interaction between  $^{31}\text{P}$  nuclei and surrounding electrons that shift the resonance frequency  $f_0 = 80.143\text{ MHz}$  to the slightly larger value,  $f \sim 80.166\text{ MHz}$ . We obtain the Knight shift  $^{31}\text{K}$  for each temperature by using the formula  $^{31}\text{K} = (f - f_0)/f_0 \times 100\%$ , where  $f$  is the peak frequency of the lineshape. The temperature dependence of  $^{31}\text{K}$  is plotted in Fig. 5(a).  $^{31}\text{K}$  of LiFeP is only  $\sim 0.03\%$ , which is much smaller than the  $^{75}\text{K} \sim 0.18\%$  at  $^{75}\text{As}$  of LiFeAs [26, 27] and NaFeAs [28]. More interestingly,  $^{31}\text{K}$

hardly changes in the measured temperature range. This situation is different from the case of  $^{75}\text{K}$  of LiFeAs, where  $^{75}\text{K}$  smoothly decreases with the decreasing temperature [26, 27].

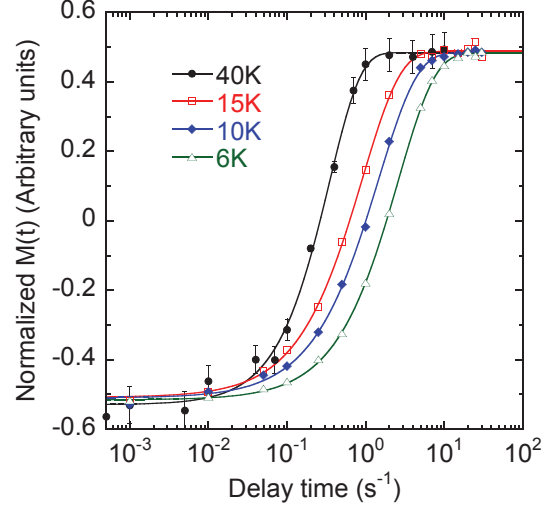


Fig. 4: (Color online) Typical nuclear spin recovery curves  $M(t)$  after an inversion pulse for  $^{31}\text{P}$ . Solid curves represent appropriate fits to determine  $T_1$  with the stretched exponential time dependence.

To obtain the insight of the spin dynamics, we measure the spin-lattice relaxation rate  $\frac{1}{T_1}$  at the peak frequency of  $^{31}\text{P}$  NMR lines.  $T_1$  represents the time scale during which the nuclear spins return to its thermal equilibrium after the absorption of the inverted radio-frequency pulse. The recovery of the nuclear magnetization after the inversion pulse,  $M(t)$ , was fitted to a stretched exponential equation,  $M(t) = M_0[1 - A \exp[-(t/T_1)^\alpha]]$  where  $M_0, A, T_1$  and  $\alpha$  are the free parameters. We show typical nuclear spin recovery curves of the LiFeP sample for  $^{31}\text{P}$  site in Fig. 4. The exponent  $\alpha$  varies smoothly from  $\sim 1.0$  at 280 K to  $\sim 0.9$  at 4.2 K. Theoretically, the spin contribution to  $\frac{1}{T_1}$  may be written using the imaginary part of the dynamical electron spin susceptibility  $\chi''(\mathbf{q}, f)$  as [29],

$$\frac{1}{T_1} = \frac{2\gamma_n^2 k_B T}{g^2 \mu_B^2} \sum_{\mathbf{q}} |A(\mathbf{q})|^2 \frac{\chi''(\mathbf{q}, f)}{f}, \quad (1)$$

where  $A(\mathbf{q})$  is the hyperfine form factor [29] and  $f$  the measured frequency.  $T_1$  can be as long as  $\sim 250$  seconds for non-magnetic insulators such as the direct gap semiconductor LiZnP, and become five orders shorter to  $\sim 2.5$  milliseconds when strong magnetic fluctuations exist [30].

We show the  $T$ -dependence of the spin-lattice relaxation rate  $\frac{1}{T_1}$  divided by  $T$ ,  $\frac{1}{T_1 T}$  in Fig. 5(b). We note that the results of  $\frac{1}{T_1 T}$  hardly change even if we fix the exponent  $\alpha$  equal to 1.0 throughout the entire temperature range. The value of  $\frac{1}{T_1 T}$  at  $^{31}\text{P}$  site of LiFeP is  $\sim 0.065\text{ s}^{-1}\text{K}^{-1}$ , which is almost an order smaller than  $\sim 0.45\text{ s}^{-1}\text{K}^{-1}$  at  $^{75}\text{As}$  sites of LiFeAs [16, 26, 27, 31], implying much weaker

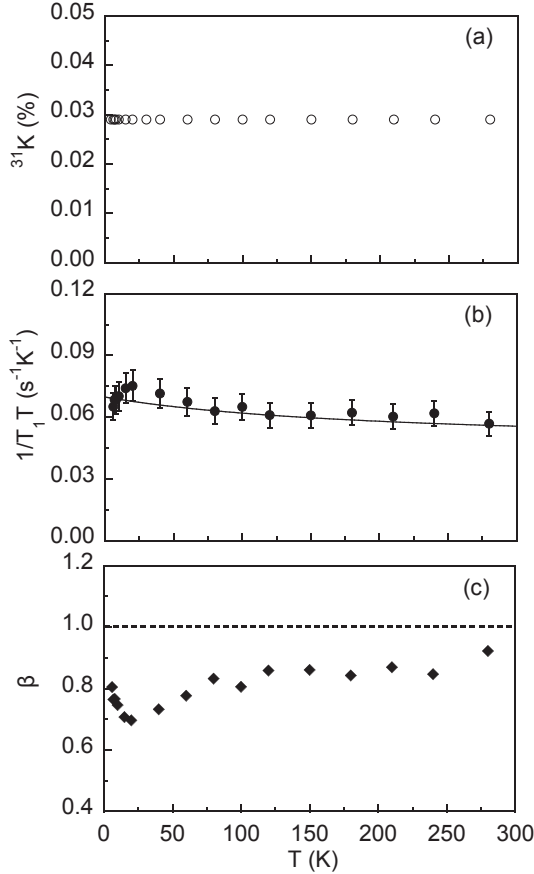


Fig. 5: (a) The temperature dependence of  $^{31}\text{P}$  NMR Knight shifts. (b)  $T$ -dependent  $\frac{1}{T_1T}$  for LiFeP. The solid line is a guide for eyes. (c) The plot of Korringa factor  $\beta$  versus temperature; Horizontal dotted line indicates an expected value  $\beta = 1$  for noninteracting electrons.

spin fluctuations in the LiFeP system. This result also indicates that the electron correlation is much weaker in LiFeP than LiFeAs, and is consistent with significant mass enhancement in LiFeAs than LiFeP observed in high field quantum oscillations [32]. In addition, we find that  $\frac{1}{T_1T}$  display a slight enhancement toward the low temperature. This feature is qualitatively similar to the case of LiFeAs [16], indicating that antiferromagnetic spin fluctuations do exist in LiFeP although they are weaker.

We can also use the Korringa relation,  $T_1TK_s^2 = \frac{\hbar}{4\pi k_B} \frac{\gamma_e^2}{\gamma_n^2} \beta$ , to evaluate quantitatively the strength of the electron correlations. Where  $\gamma_e$  and  $\gamma_n$  are the electron and nuclear gyromagnetic ratios, respectively.  $K_s$  is the spin susceptibility extracted from the Knight shift data in Fig. 5(a). The Korringa factor  $\beta$  reflects the magnitude of spin correlations [33]. Usually  $\beta$  is equal to 1 for a non-interacting system, and strong ferromagnetic correlations give  $\beta \gg 1$ , while strong antiferromagnetic correlations give  $\beta \ll 1$ . We show the calculated  $\beta$  in Fig. 5(c). The values of  $\beta$  in the whole measured temperature range are smaller than 1, indicating the existence of the antiferro-

magnetic fluctuations in LiFeP.  $\beta$  is close to 1, which is much larger than  $\beta \sim 0.2 \sim 0.5$  in LiFeAs [27,31], again indicating that the weaker spin correlations in LiFeP.

A close inspection of the  $\frac{1}{T_1T}$  curve indicates that a small hump appears at  $T \sim 20$  K, suggesting some magnetic instabilities exist around this temperature. Currently we do not know the origin of this magnetic instability since no anomalies have been detected around this temperature in both dc magnetic susceptibilities and the electrical resistivity. A brave assumption is that this hump is related to the SDW magnetic transition which has been absent in LiFeP and LiFeAs. A possible scenario is that Li concentrations affects the ground state of  $\text{Li}_{1\pm\delta}\text{FeP}$ , and a precise controlling of Li concentration may unveil this mystery.

**Summary and Conclusion.** – In summary, we investigated the static and dynamic spin susceptibility of the superconducting LiFeP in the paramagnetic state by NMR measurement at  $^{31}\text{P}$  site. Through the measurement of electrical resistivity, Knight shift and  $\frac{1}{T_1T}$ , we found that  $\rho \sim T^2$ ,  $^{31}\text{P}K \sim \text{constant}$  and Korringa ratio  $\beta \sim 0.8$ , which all point to the weak spin correlations in LiFeP. Our results indicate that the antiferromagnetic spin fluctuations are slightly enhanced toward  $T_c$  although their magnitudes are much weaker than those of LiFeAs. This on one hand indicates that antiferromagnetic fluctuations are important for the superconductivity in LiFeP, and on the other hand may explain the much lower  $T_c$  of LiFeP than that of LiFeAs. We also detected an magnetic instability around  $\sim 20$  K, which may be related to the different ground states arising from Li off-stoichiometry. We are applying electrochemical method to precisely control the amount of Li concentration in LiFeP and LiFeAs to elucidate their mysterious ground states.

\*\*\*

The work at was supported by National Basic Research Program of China (No.2011CBA00103, 2014CB921203), NSF of China (No.11274268).

## REFERENCES

- [1] KAMIHARA Y., WATANABE T., HIRANO M., AND HOSONO H., *J. Am. Chem. Soc.*, **130** (2008) 3296.
- [2] KAMIHARA Y., HIRAMATSU H., HIRANO M., KAWAMURA R., YANAGI H., KAMIYA T., AND HOSONO H., *J. Am. Chem. Soc.*, **128** (2006) 10012.
- [3] ROTTER M., TEGEL M., AND JOHRENDT D., *Phys. Rev. Lett.*, **101** (2008) 107006.
- [4] WANG X. C., LIU Q. Q., LV Y. X., GAO W. B., YANG L. X., YU R. C., LI F. Y., AND JIN C. Q., *Solid State Commun.*, **148** (2008) 538.
- [5] HSU F.-C., LUO J.-Y., YEH K.-W., CHEN T.-K., HUANG T.-W., WU P. M., LEE Y.-C., HUANG Y.-L., CHU Y.-Y., YAN D.-C., AND WU M.-K., *Proc. Nat. Acad. Sci.(USA)*, **105** (2008) 14262.

- [6] ZHU X. Y., HAN F., MU G., CHENG P., SHEN B., ZENG B., AND WEN H. H., *Phys. Rev. B*, **79** (2009) 220512(R).
- [7] SHIRAGE P. M., KIHOU K., LEE C. H., KITO H., EISAKI H., AND IYO A., *J. Am. Chem. Soc.*, **133** (2011) 9630.
- [8] STEWART G. R., *Rev. Mod. Phys.*, **83** (2011) 1589.
- [9] ISHIDA K., NAKAI Y., AND HOSONO H., *J. Phys. Soc. Jpn.*, **78** (2009) 062001.
- [10] DENG Z., WANG X. C., LIU Q. Q., ZHANG S. J., LV Y. X., ZHU J. L., YU R. C., AND JIN C. Q., *Europhys. Lett.*, **87** (2009) 37004.
- [11] WANG X. C., LIU Q. Q., LV Y. X., GAO W. B., YANG L. X., YU R. C., LI F. Y., AND JIN C. Q., *Solid State Commun.*, **148** (2008) 538.
- [12] PARKER D. R., PITCHER M. J., BAKER P. J., FRANKE I., LANCASTER T., BLUNDELL S. J., AND CLARKE S. J., *Chem. Comm.*, **16** (2009) 2189.
- [13] HASHIMOTO K., KASAHARA S., KATSUMATA R., MIZUKAMI Y., YAMASHITA M., IKEDA H., TERASHIMA T., CARRINGTON A., MATSUDA Y., AND SHIBAUCHI T., *Phys. Rev. Lett.*, **108** (2012) 047003.
- [14] KITAGAWA K., MEZAKI Y., MATSUBAYASHI K., UWATOKO Y., AND TAKIGAWA M., *J. Phys. Soc. Jpn.*, **80** (2011) 033705.
- [15] KLANJŠEK M., JEGLIČ P., LV B., GULOY A. M., CHU C. W., AND ARČON D., arXiv:1011.1387v1 (2010).
- [16] MA L., ZHANG J., CHEN G. F., AND YU W. Q., *Phys. Rev. B*, **82** (2010) 180501(R).
- [17] NING F. L., AHILAN K., IMAI T., SEFAT A. S., MCGUIRE M. A., SALES B. C., MANDRUS D., CHENG P., SHEN B., AND WEN H. H., *Phys. Rev. Lett.*, **104** (2010) 037001.
- [18] NAKAI Y., IYE T., KITAGAWA S., ISHIDA K., IKEDA H., KASAHARA S., SHISHIDO H., SHIBAUCHI T., MATSUDA Y., AND TERASHIMA T., *Phys. Rev. Lett.*, **105** (2010) 107003.
- [19] IMAI T., AHILAN K., NING F. L., MCQUEEN T. M., AND CAVA R. J., *Phys. Rev. Lett.*, **102** (2009) 177005.
- [20] OKA T., LI Z., KAWASAKI S., CHEN G. F., WANG N. L., AND ZHENG G. Q., *Phys. Rev. Lett.*, **108** (2012) 047001.
- [21] KINOCHI H., MUKUDA H., YASHIMA M., KITAOKA Y., SHIRAGE P. M., EISAKI H., AND IYO A., *Phys. Rev. Lett.*, **107** (2011) 047002.
- [22] WAUTELET M., GÉRARD A., GRANDJEAN F., STROOPER K. DE, AND ROBBRECHT G., *Phys. Stat. Sol. (a)*, **39** (1977) 425.
- [23] MYDEEN K., LENGYE E., DENG Z., WANG X. C., JIN C. Q., ANDX NICKLAS C. Q., *Phys. Rev. B*, **82** (2010) 014514.
- [24] BŁACHOWSKI A., RUEBENBAUER K., ŻUKROWSKI J., PRZEWOŹNIK J., AND MARZEC J., *J. Alloys Compd.*, **505** (2010) 35.
- [25] KASAHARA S., HASHIMOTO K., IKEDA H., TERASHIMA T., MATSUDA Y., AND SHIBAUCHI T., *Phys. Rev. B*, **85** (2012) 060503(R).
- [26] BAEK S. H., GRAFE H. J., HAMMERATH F., FUCHS M., RUDISCH C., HARNAGEA L., ASWARTHAM S., WURMEHL S., BRINK J. VAN DEN, AND BÜCHNER B., arXiv:1108.2592 (2011).
- [27] LI Z., OOE Y., WANG X. C., LIU Q. Q., JIN C. Q., ICHIOKA M., AND ZHENG G. Q., *J. Phys. Soc. Jpn.*, **79** (2010) 083702.
- [28] KITAGAWA K., MEZAKI Y., MATSUBAYASHI K., UWATOKO Y., AND TAKIGAWA M., *J. Phys. Soc. Jpn.*, **80** (2011) 033705.
- [29] MORIYA T., *J. Phys. Soc. Jpn.*, **18** (1963) 516.
- [30] DING C., QIN C., MAN H. Y., IMAI T., AND NING F. L., *Phys. Rev. B*, **88** (2013) 041108(R).
- [31] JEGLIČ P., POTOČNIK A., KLANJŠEK M., BOBNAR M., JAGODIČ M., KOCH K., ROSNER H., MARGADONNA S., LV B., GULOY A. M., AND ARČON D., *Phys. Rev. B*, **81** (2010) 140511(R).
- [32] PUTZKE C., COLDEA A. I., GUILLAMÓN I., VIGNOLLES D., MCCOLLAM A., LEBOEUF D., WATSON M. D., MAZIN I. I., KASAHARA S., TERASHIMA T., SHIBAUCHI T., MATSUDA Y., AND CARRINGTON A., *Phys. Rev. Lett.*, **108** (2012) 047002.
- [33] PENNINGTON C. H., AND STENGER V. A., *Rev. Mod. Phys.*, **68** (1996) 855.